

# Single-Molecule Analysis Demonstrates Stress-Enhanced Binding between *Staphylococcus aureus* Surface Protein IsdB and Host Cell Integrins

Marion Mathelié-Guinlet, Felipe Viela, Mariangela Jessica Alfeo, Giampiero Pietrocola, Pietro Speziale, and Yves F. Dufrêne\*

Cite This: *Nano Lett.* 2020, 20, 8919–8925

Read Online

ACCESS |

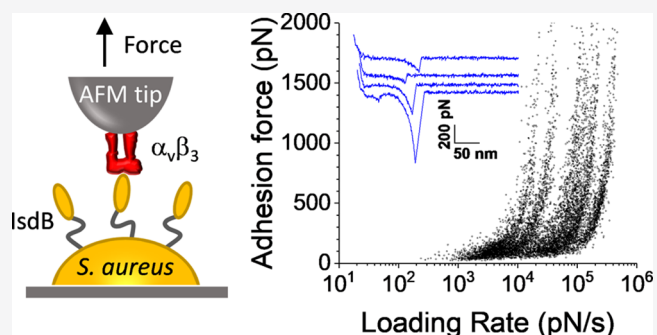
Metrics & More

Article Recommendations

Supporting Information

**ABSTRACT:** Binding of *Staphylococcus aureus* surface proteins to endothelial cell integrins plays essential roles in host cell adhesion and invasion, eventually leading to life-threatening diseases. The staphylococcal protein IsdB binds to  $\beta_3$ -containing integrins through a mechanism that has never been thoroughly investigated. Here, we identify and characterize at the nanoscale a previously undescribed stress-dependent adhesion between IsdB and integrin  $\alpha_v\beta_3$ . The strength of single IsdB– $\alpha_v\beta_3$  interactions is moderate ( $\sim 100$  pN) under low stress, but it increases dramatically under high stress ( $\sim 1000$ – $2000$  pN) to exceed the forces traditionally reported for the binding between integrins and Arg-Gly-Asp (RGD) sequences. We suggest a mechanism where high mechanical stress induces conformational changes in the integrin from a low-affinity, weak binding state to a high-affinity, strong binding state. This single-molecule study highlights that direct adhesin–integrin interactions represent potential targets to fight staphylococcal infections.

**KEYWORDS:** staphylococcal adhesion, IsdB,  $\alpha_v\beta_3$  integrins, single-molecule, binding strength, catch bond



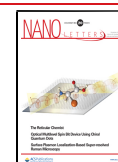
*Staphylococcus aureus* is an opportunistic pathogen which can lead to life-threatening diseases, such as bloodstream infections.<sup>1–3</sup> Mostly known for its role in nosocomial infections and for its ability to resist methicillin, *S. aureus* is now considered as a worldwide clinical problem.<sup>4</sup> *S. aureus* expresses and uses a range of cell wall-anchored (CWA) proteins to mediate adhesion to extracellular matrix (ECM) components of endothelial cells. While it has long been thought to be an extracellular pathogen, there is now compelling evidence that this pathogen uses such CWA proteins to support invasion of epithelial and endothelial cells.<sup>5–8</sup>

Integrins are heterodimeric mammalian transmembrane receptors mediating adhesion to the ECM or to other cells.<sup>9</sup> Ligand binding provides mechanical cues and triggers biochemical signals to regulate a number of physiological functions such as cell development, cytoskeleton organization, and surface receptor clustering. Fibronectin-binding proteins (FnBPs) of *S. aureus* interact with  $\alpha_3\beta_1$  integrins indirectly through fibronectin (Fn) of the ECM, which acts as a molecular bridge tethering the pathogen to the target cell and promoting its internalization.<sup>8,10,11</sup> Similarly, vascular endothelial dysfunction has been attributed to the ability of *S. aureus* clumping factor A (ClfA) to adhere to  $\alpha_v\beta_3$  integrins expressed on endothelial cells, with a critical role of fibrinogen

(Fig).<sup>12</sup> Though less investigated, some pathogens can also interact directly with host integrins, as exemplified by enteropathogenic *Yersinia pseudotuberculosis* adhering and invading epithelial cells via  $\beta_1$  integrins binding to invasin YadA.<sup>13,14</sup> As integrins are potential targets to treat *S. aureus* bloodstream infections, understanding their interactions with adhesins is an important topic.

The surface determinant IsdB protein binds to hemoglobin and provides *S. aureus* bacteria with a source of iron.<sup>15</sup> It has also been shown to promote the adhesion to platelets via direct binding to  $\alpha_{IIb}\beta_3$  and potentially to some other  $\beta_3$ -containing integrins.<sup>16–19</sup> Among them,  $\alpha_v\beta_3$  is the major integrin expressed on endothelial cells.<sup>9</sup> These integrins promote bacterial adhesion to the ECM thanks to their multiligand binding activities (Vitronectin, Fn, Fg).<sup>20</sup> Vitronectin is notably known to form a molecular bridge between surface-exposed IsdB and  $\alpha_v\beta_3$  integrins, but invasion of HeLa and

**Received:** October 7, 2020  
**Revised:** November 16, 2020  
**Published:** November 25, 2020



HUVEC cells by *S. aureus* also occurs, though with lower probability, in the absence of vitronectin, suggesting that a direct adhesion–integrin interaction might occur and contribute to *S. aureus* pathogenesis.<sup>21</sup> Here, we use single-molecule experiments to demonstrate direct binding of IsdB to  $\alpha_V\beta_3$  and to decipher the molecular forces and dynamics guiding such interactions. The mechanical stability of the IsdB– $\alpha_V\beta_3$  complex is low under low stress conditions (150 pN at a loading rate  $< 10^2$  pN/s) but is strongly increased by mechanical tension (up to 2000 pN at a loading rate of  $10^5$  pN/s). Reminiscent of a catch bond behavior, this force-enhanced binding of IsdB to  $\alpha_V\beta_3$  integrin might help the pathogen to firmly attach to host cells and resist fluid shear stress conditions that, in turn, translate into higher tensile loads on adhesive bonds.

## RESULTS AND DISCUSSION

**IsdB Supports Bacterial Adhesion to Immobilized  $\alpha_V\beta_3$  Integrins.** We first determined the adhesion forces between single *S. aureus* WT bacteria (exposing IsdB adhesins) and  $\alpha_V\beta_3$ -coated substrates. Figure 1A shows the maximum adhesion forces and rupture lengths histograms obtained for three representative cells. High binding probability was frequently observed between WT cells and  $\alpha_V\beta_3$  surfaces ( $40 \pm 5\%$  from those three representative cells) with adhesion forces exhibiting a widely spread distribution, from 50 pN to 1500 pN (Figure 1A). Only specific adhesive events, showing defined single peaks, well fitted by the worm-like chain model, were considered in the analysis; this means that non-specific adhesion arising, e.g., from other proteins or biomolecules unspecifically interacting with integrins were discarded. All cells showed major adhesion forces below 500 pN, with a mean force of  $153 \pm 106$  pN (mean  $\pm$  s.d. on  $n = 291$  adhesive curves from 3 cells; frequency of 74%). Larger forces up to 1500 pN were also observed in 26% of the cases. It is noteworthy that we observed rupture lengths of  $112 \pm 55$  nm ( $n = 392$  events from 3 cells). Given that the IsdB adhesin is made of  $\sim 600$  residues and that each amino acid contributes to 0.36 nm of the contour length, the fully unfolded protein should be  $\sim 215$  nm, larger than the reported rupture lengths. Consequently, the observed bonds break before the complete unfolding of IsdB, highlighting the mechanical stability of those *S. aureus* adhesins.

The specificity of interaction was tested by measuring the forces between IsdB<sup>−</sup> cells lacking IsdB and  $\alpha_V\beta_3$ -coated substrates (Figure 1B). There was a significant drop in adhesion probability, from  $35 \pm 7\%$  (14 WT cells, Figure 3A) to  $22 \pm 9\%$  (12 IsdB<sup>−</sup> cells, Figure 3A), and only low forces of  $142 \pm 87$  pN ( $n = 155$  adhesive events from 3 independent cells) were observed, suggesting that IsdB plays a critical role in the measured interaction forces. The residual adhesion still observed for IsdB<sup>−</sup> cells might arise from other surface receptors. Nonetheless, as reported below, the single molecule configuration leads to almost no adhesion for mutant cells, confirming our hypothesis on the critical and specific role of IsdB in driving binding to  $\alpha_V\beta_3$  integrin. Moreover, there was a strong reduction of adhesion when blocking the integrin with either anti- $\alpha_V\beta_3$  antibodies or cilengitide, with low and high forces still being observed (Figure 1C and D, Figure 3A). The binding probability dropped from  $35 \pm 7\%$  for WT cells to  $15 \pm 6\%$  (16 cells) and  $23 \pm 9\%$  (13 cells) for WT cells treated with antibodies and cilengitide, respectively. The substantial drop in adhesion confirms the overall blocking of the

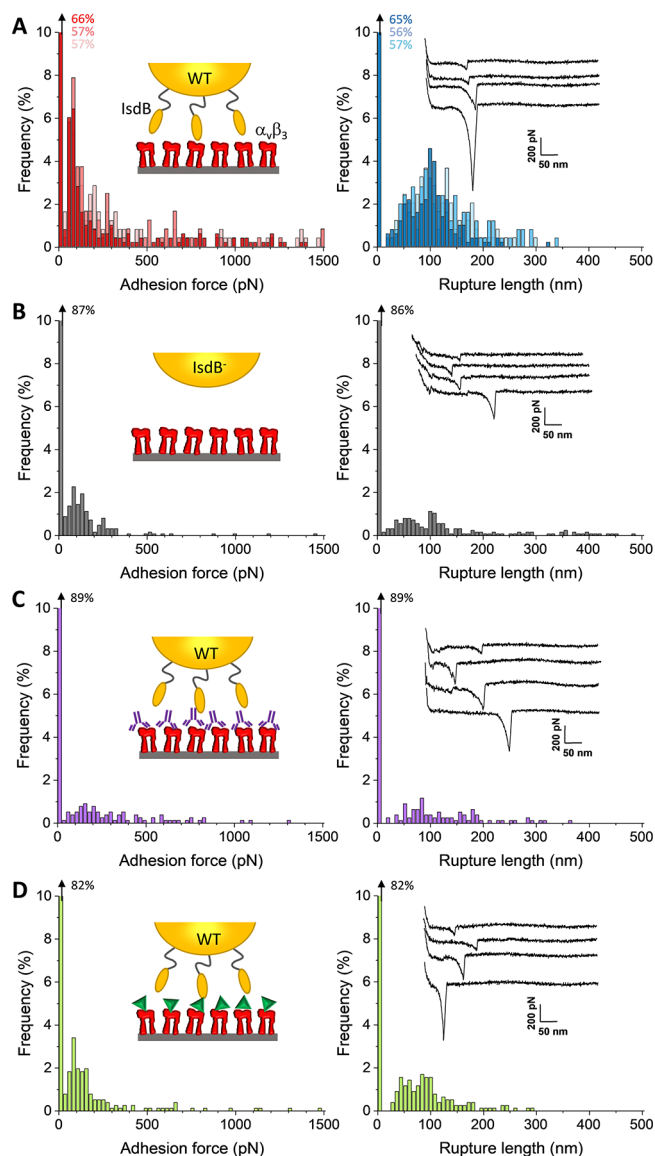


**Figure 1.** Single-cell force spectroscopy identifies IsdB as a mediator for *S. aureus* adhesion to  $\alpha_V\beta_3$  surfaces. (A) Adhesion force (left) and rupture length (right) histograms obtained between three representative WT cells and  $\alpha_V\beta_3$ -substrates interacting in PBS (color-coded). (B) Data obtained between IsdB<sup>−</sup> cells (3 merged cells), lacking the IsdB adhesins, and  $\alpha_V\beta_3$ -substrates. (C, D) Data obtained between WT cells (3 merged cells) and  $\alpha_V\beta_3$ -substrates blocked with anti- $\alpha_V\beta_3$  antibodies LM 609 and cilengitide, respectively. For each panel, the left inset represents a scheme of the setup and the right inset shows representative retraction profiles. A contact time of 500 ms, a maximum applied force of 250 pN, and approach and retraction speeds of 1000 nm/s were used to record force–distance curves from which adhesion forces and rupture lengths were extracted.

interaction between IsdB and  $\alpha_V\beta_3$ , though residual specific binding can still occur.

**Strength of Single IsdB– $\alpha_V\beta_3$  Interactions.** To further quantify the strength of single IsdB– $\alpha_V\beta_3$  interactions, we measured the forces between  $\alpha_V\beta_3$  integrins grafted on the AFM tip and *S. aureus* WT bacteria (Figure 2A). Similar to single-cell measurements, we observed the most probable adhesion forces below 500 pN, centered at  $175 \pm 121$  pN (mean  $\pm$  s.d., from  $n = 193$  adhesive events from 3

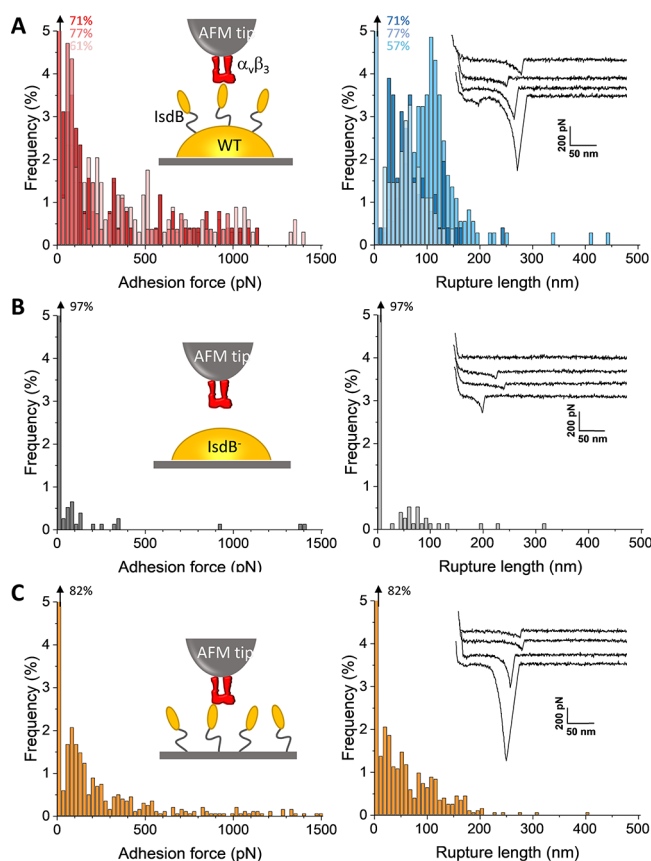


**Figure 2.** Single-molecule force spectroscopy captures the binding strength of  $\alpha_v\beta_3$  interacting with single IsdB adhesin expressed on *S. aureus*. (A) Adhesion force (left) and rupture length (right) histograms obtained on three representative WT cells probed with  $\alpha_v\beta_3$ -functionalized AFM tips (color-coded). (B) The same data on IsdB<sup>-</sup> cells (3 cells merged). (C) The same data obtained between AFM tips labeled with  $\alpha_v\beta_3$  integrins and IsdB-coated N1–N2 substrates. For each panel, the left inset represents a scheme of the setup and the right inset shows representative retraction profiles. A contact time of 500 ms, a maximum applied force of 250 pN, and approach and retraction speeds of 1000 nm/s were used to record force–distance curves from which adhesion forces and rupture lengths were extracted.

representative independent cells), in agreement with the strength of single integrins.

Again, we also observed higher forces up to 1500 pN at a frequency of 29%. Similar features, though with lower adhesion probability, were obtained when decreasing the density of integrins grafted on the tip (1% vs 10% carboxyl-terminated thiols) (Supplementary Figure S1A and S1B), suggesting that such differences in strength cannot be accounted for multiple bonds breaking in parallel but rather by intrinsic properties of the formed IsdB– $\alpha_v\beta_3$  complex. Both weak and strong interactions were abolished when probing IsdB<sup>-</sup> cells (5% vs 23% for WT cells, Figure 3B; Figure 2B), confirming that IsdB interacts specifically with  $\alpha_v\beta_3$  integrins.

Also, recombinant IsdB N1–N2 region proteins showed the same binding features as WT cells when probed against  $\alpha_v\beta_3$  tips (Figure 2C, Figure 3B), supporting the idea that IsdB was the only surface molecule involved in the interaction.

**IsdB– $\alpha_v\beta_3$  Interaction Is Strengthened by Mechanical Force.** It has been recently shown that staphylococcal adhesive interactions can be reinforced by mechanical stress.<sup>22–25</sup> When

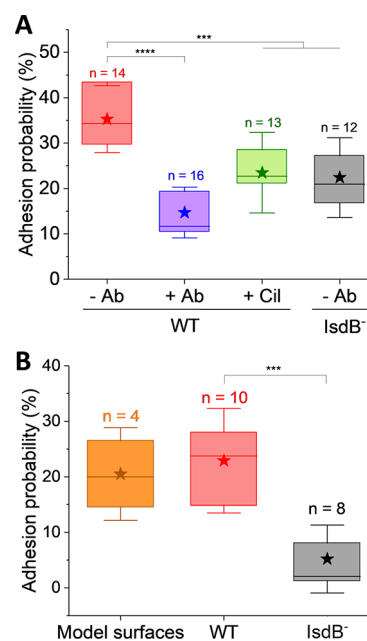


**Figure 3.** Single-cell and single-molecule force spectroscopy experiments reveal the specific binding between IsdB and  $\alpha_v\beta_3$ . (A) Box plots of the adhesion probability obtained between bacteria, either WT or mutant cells ( $n$  cells), and  $\alpha_v\beta_3$  immobilized on solid substrates, in single-cell experiments. Cil. stands for the blocking experiments performed with cilengitide and Ab for antibodies. (B) Adhesion probability for both strains and model surfaces obtained in single-molecule experiments over  $n$  independent samples. Stars account for the mean values, boxes the 25–75% quartiles, and whiskers the standard deviation. Student's  $t$ -tests: \*\*\*\* $p$  < 0.0001 and \*\*\* $p$  < 0.001.

the bacteria adhere to a surface through the specific interaction between an adhesin and its ligand, this interaction is under tensile load due to the diverse flow conditions encountered in the environment. Increasing shear stress thus translates into increasing tensile load on the bond. Therefore, we used dynamic force spectroscopy (DFS) to measure the rupture force ( $F$ ) between  $\alpha_v\beta_3$  tips and WT cells, when the complex is pulled at different speeds, i.e., at different loading rates (LRs) assessed from the force versus time curves (Figure 4). Increasing the retraction speed from 0.5  $\mu\text{m/s}$  to 10  $\mu\text{m/s}$  led to a shift toward higher forces, with a progressive depletion of the main force population at  $\sim 100$  pN and an increase in the amount of higher forces both below and above 500 pN (Figure 4A), suggesting a force-enhanced interaction. Figure 4B shows the resulting dynamic force spectroscopy plot pooled from four independent cells. Clearly, a nonlinear behavior was observed with forces rising up to 2000 pN at LR higher than  $10^4$  pN/s. Overall, the whole set of forces could not be fitted by the Bell–Evans or the Friddle–Noy–de Yoreo (FNdeY) models.<sup>26,27</sup> Nonetheless, the low force regime at  $\sim 100$  pN could be described by a FNdeY model, but the sudden increase in force and the increasing proportion of forces higher than 500 pN at higher loading rates were beyond the expectation of this model. This led us to believe that such strong bonds arised from a force-induced deformation and conformational change in the complex. We analyzed the distribution of binding forces over discrete ranges of LRs (Figure 4C,  $n = 7774$  adhesion events over four cells; see also Supplementary Figure S2). The lowest LRs ( $10^3 < \text{LR} < 3 \times 10^3$  pN/s) showed only weak forces of 100–200 pN while the highest LRs ( $10^5 < \text{LR} < 3 \times$

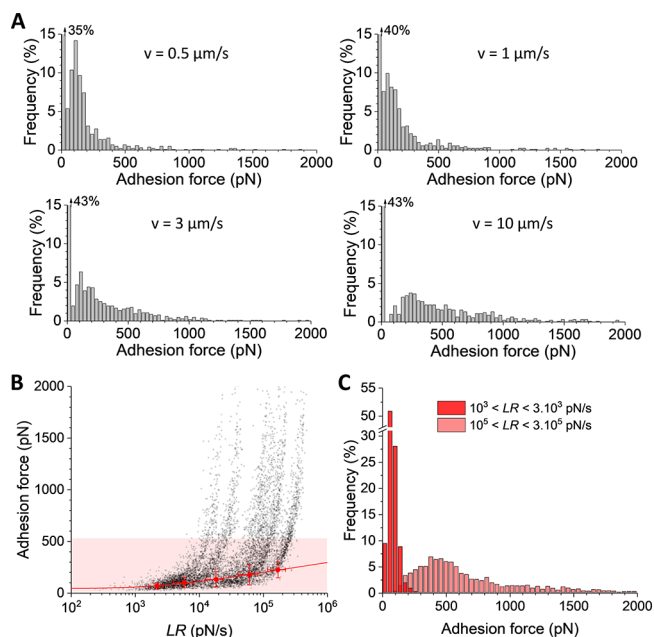


**Figure 4.** Mechanical load enhances the IsdB- $\alpha_v\beta_3$  interaction strength. (A) Adhesion force histograms, obtained at different retraction speeds, by recording force curves on one representative WT cell using AFM tips labeled with  $\alpha_v\beta_3$  integrins. (B) Dynamic force spectroscopy plot (force,  $F$ , vs loading rate,  $LR$ ) for the IsdB- $\alpha_v\beta_3$  interaction on four independent cells (pooled from  $n = 7774$  adhesive events). The red zone indicates the threshold between the low force regime ( $F < 500$  pN) and the high regime ( $F > 500$  pN). Shown in red is a Friddle–Noy–de Yoreo fit, with an equilibrium force  $F_{eq} = 44 \pm 15$  pN, a transition energetic barrier at  $x_\beta = 0.100 \pm 0.002$ , and an off-rate constant of dissociation  $k_{off}^0 = 30.6 \pm 18.4$  s $^{-1}$ . (C) Adhesion force histograms obtained by sorting the DFS data in discrete  $LR$  ranges.

$10^5$  pN/s) featured stronger forces in the 500 pN range and up to 2000 pN. At intermediate  $LR$ s, both populations of forces were observed in different proportions depending on the  $LR$  (Supplementary Figure S2). The DFS plot obtained while lowering the integrin density on the tip exhibited similar features with forces up to 2000 pN at  $LR$ s higher than  $10^4$  pN/s and had both increasing proportion of higher forces and stronger forces with increasing  $LR$ s (Supplementary Figure S1C). Consequently, it is rather unlikely that multiple cumulative bonds could explain such high forces never reported before for a direct adhesin–integrin binding.

Staphylococci have evolved dedicated mechanisms to mediate strong attachment to host cells under shear stress, chiefly mediated by surface-exposed proteins specifically binding to host receptors or ECM proteins.<sup>28,29</sup> We have shown here that the direct interaction between IsdB and  $\alpha_v\beta_3$  integrin is stress sensitive, becoming extraordinarily strong (1000–2000 pN) under high stress conditions. Such interaction strength is equivalent to that of a covalent bond and is thus much higher than that of classical ligand–integrin bonds studied so far, in the range of  $\sim 100$  pN.<sup>30–32</sup>

Earlier studies have revealed the capacity of integrins to form such force-enhanced complexes with, e.g., Fn, inducing a strengthening of cellular adhesion. Notably, based on single-molecule experiments, Kong et al. observed an increase in bond lifetimes with forces ranging from 10 to 30 pN for a Fn fragment in complex with an integrin fusion protein.<sup>33</sup> Also, Strohmeier et al. found that fibroblasts initiate binding to Fn

through adhesive complexes with  $\alpha_5\beta_1$  integrins that are strengthened, in terms of force and lifetime, to resist shear conditions.<sup>34</sup> While these studies provide compelling evidence that integrin-mediated adhesion of mammalian cells is modulated by mechanical force, whether this occurs directly between integrins and bacterial adhesins was not known. Solving this question is yet critical to the development of new integrin inhibitors to treat *S. aureus* infections. Unique to our study is that IsdB directly binds to  $\alpha_v\beta_3$ , in the absence of any ligands of the ECM, and that the interaction is extraordinarily strong under high stress conditions (loading rate of  $10^5$  pN/s). This strong adhesion could not be described by the Friddle–Noy–de Yoreo model, pointing to an unusual force-activated binding mechanism. Our force-strengthened adhesion is comparable with that reported for dock, lock, and latch (DLL) complexes<sup>35,36</sup> such as staphylococci SdrG, ClfA, and ClfB adhesins<sup>37–40</sup> that can resist extreme forces  $\sim 2$  nN because of an intricate hydrogen-bonding network formed by the locked peptide and the adhesin binding pocket.<sup>39</sup> Though involving a different binding mechanism, such a force-dependent hydrogen-bonding network might contribute to the ultrastrong IsdB- $\alpha_v\beta_3$  interaction observed here.

Moreover, our force-enhanced IsdB- $\alpha_v\beta_3$  interaction is reminiscent of the catch bond behavior exhibited by the blood proteins selectins<sup>41</sup> and the bacterial adhesin FimH,<sup>42–44</sup> which become longer lived with increasing shear stress. This phenomenon has also been previously reported for some ligand–integrin complexes that, in turn, strengthen cellular adhesion under stress.<sup>45–49</sup> Interestingly, theoretical analyses have revealed that external load could induce an increase in the lifetime of hydrogen bonds, formed in the binding pocket between a receptor and its ligand, leading to a catch bond behavior,<sup>50</sup> a finding that also explains how structurally unrelated integrin–Fn and/or actomyosin complexes bind.

Although the molecular origin of IsdB- $\alpha_v\beta_3$  interaction remains unclear, we suggest a model in which force-induced structural changes upshift the integrins to a high affinity state. This notion is supported by previous works showing that *S. aureus* adheres to platelets through the binding of IsdB to the high affinity form of platelet integrins  $\alpha_{IIb}\beta_3$ , without the need of an extra ECM protein.<sup>16,17</sup> Inhibition of  $\alpha_v\beta_3$  adhesion by cilengitide observed in this work also highlights that the integrin binding site for cilengitide and IsdB must be close and that this proximity reduces binding of IsdB, as IsdB does not contain any RGD sequence. In addition, it is possible that force acting on integrins is transmitted to the IsdB binding site, leading to a conformational change of the adhesin and creating a new hydrogen-bonding network that stabilizes the complex. Overall, our single-molecule approach on purified integrins provides a crucial initial understanding of the molecular mechanism underlying the direct binding of bacterial adhesins to such targets, without the requirement of ECM proteins. Further work is needed to confirm whether similar direct IsdB- $\alpha_v\beta_3$  interaction occurs on endothelial cells. The force-enhanced adhesion between IsdB and integrins might be one among many mechanisms staphylococci have developed to efficiently colonize and/or invade their hosts while resisting shear forces encountered in various environments upon infection.<sup>51</sup>

## METHODS

**Bacterial Strains and Growth Conditions.** *S. aureus* SH1000 WT (expressing IsdB) and IsdB $^-$  mutant (lacking the

adhesin) cells were cultured in brain heart infusion (BHI) broth overnight at 37 °C and under shaking at 200 rpm. When the stationary phase was reached, bacteria were diluted 100× and grown in RPMI (Roswell Park Memorial Institute medium, usually used for mammalian cell culture) overnight (37 °C, 200 rpm) to create iron-restricted conditions. Cells were finally harvested three times by centrifugation at 3000g for 5 min. They were diluted 100× in PBS and used directly for AFM experiments.

**AFM Tips and Gold Surfaces Functionalization with Integrin  $\alpha_V\beta_3$ .** Gold-coated glass coverslips and gold-coated OMCL-TR4 AFM cantilevers (Olympus, Ltd., Tokyo, Japan) were immersed overnight in an ethanolic solution containing 16-mercaptododecahexanoic acid (0.1 mM) and 1-mercapto-1-undecanol (0.9 mM). They were then washed with ethanol and dried under a stream of N<sub>2</sub>. Substrates and AFM cantilevers were then immersed for 30 min in a solution of *N*-hydroxysuccinimide (NHS, 10 mg/mL) and 1-ethyl-3-(3-dimethylaminopropyl)-carbodiimide (EDC, 25 mg/mL). The resulting NHS–carboxyl ester-exposing cantilevers and substrates were rinsed with ultrapure water and incubated with  $\alpha_V\beta_3$  integrin (0.1 mg/mL; Sigma) for 1 h. Finally, they were rinsed with PBS buffer and stored in PBS before AFM experiments.

**Single-Cell Force Spectroscopy Experiments.** The preparation of colloidal probes for single-cell experiments was described previously, and the cell viability, after attachment to the probe, was validated.<sup>52</sup> Thanks to an optical microscope coupled to the AFM instrument (Nanowizard III and IV atomic force microscopes, JPK Instruments), a triangular tipless cantilever (NP-O10, Bruker) was gently immersed in a thin layer of UV-curable glue (NOA 63, Norland Edmund Optics) and was then brought in contact with a single silica bead (6.1  $\mu$ m diameter, Bangs Laboratories) for it to attach. The resulting colloidal probes were exposed to UV light for 15 min to cure the glue. They were then coated with dopamine for 1 h by immersion in Tris-buffered saline (TBS; Tris, 50 mM; NaCl, 150 mM; pH 8.5) containing 4 mg/mL dopamine hydrochloride (Sigma-Aldrich) and further rinsed in three baths of TBS. The spring constant of the probe cantilever was determined, before attachment of the bacteria, by the thermal noise method and gave an average value of 0.085 N/m. For single-cell experiments, 50  $\mu$ L of a diluted suspension of bacteria was dropped on a polystyrene Petri dish for 20 min before being rinsed with PBS. An integrin  $\alpha_V\beta_3$ -coated substrate was placed right next to the bacteria spot, and the Petri dish was finally covered with 3 mL of PBS. One bacterium was caught electrostatically by gently approaching the colloidal probe toward an isolated cell, and verifying, on the optical cliché, its absence when the cantilever was retracted from its position. The cell probe was then brought into contact with the  $\alpha_V\beta_3$ -coated substrate to record multiple force curves (maps of 16  $\times$  16 pixels) on different spots (5  $\mu$ m  $\times$  5  $\mu$ m), with an applied force of 250 pN, approach and retraction speeds of 1  $\mu$ m/s, and a contact time of 500 ms. For blocking experiments, we used commercially available cilengitide (Sigma), and anti  $\alpha_V\beta_3$  antibody LM 609 (Abcam), 150  $\mu$ L of which were incubated on the  $\alpha_V\beta_3$ -surface for 1 h at a concentration of 0.1 mg/mL. All experiments were performed at room temperature.

**Single-Molecule Force Spectroscopy Experiments.** For single-molecule experiments, bacteria were first immobilized on a polystyrene Petri dish; a 50  $\mu$ L drop of diluted

bacterial suspension was deposited on the center of the dish and let sit for 20 min before being rinsed with PBS and immersed in 3 mL of PBS. Gold-coated OMCL-TR4 AFM cantilevers were initially calibrated on the bare polystyrene with the thermal noise method and gave an average value of  $k \sim 0.05$  N/m. Finally, the AFM-functionalized tip was brought in contact with an isolated bacterium, and adhesion maps were recorded on top of the cell (500 nm  $\times$  500 nm, 32  $\times$  32 pixels) with an applied force of 250 pN, a constant approach and retraction speed of 1  $\mu$ m/s, and a contact time of 500 ms. In some experiments, gold surfaces coated with recombinant IsdB were probed. To this end, recombinant IsdB N2–N3 (residues 48–480) was expressed from pQE30 (Qiagen, Hilden, Germany) in *E. coli* XL1-Blue (Agilent Technologies, CA, USA) and purified by Ni<sup>2+</sup>-affinity chromatography on a HiTrap chelating column (GE Healthcare, Buckinghamshire, UK) as reported in ref 21. The retraction speed was varied from 0.5 to 10  $\mu$ m/s for loading rate experiments. All experiments were performed at room temperature.

**Single-Cell and Single-Molecule Data Analysis.** We used the JPK data processing software to analyze the data. The adhesion force and rupture distance of the last specific adhesion peak for each curve were determined and then plotted as histograms in Origin. A specific adhesive event is defined as an event, occurring far from the contact point, and where the retraction segment of the force curve shows a variation in the slope (representing the stretching of the molecular complex) before the rupture point. The frequency of those specific adhesion events, recorded in a map on a 500 nm  $\times$  500 nm area, is defined as the adhesion probability. Those specific adhesive events, mainly showing a single defined peak, were well fitted with the worm-like chain model during the analysis process. Loading rate was calculated from the linear slope immediately preceding the rupture event on the force versus time curves. Student's *t*-test was used to estimate the statistical differences among the obtained results; *p* values are provided in figure captions when appropriate.

## ■ ASSOCIATED CONTENT

### Supporting Information

The Supporting Information is available free of charge at <https://pubs.acs.org/doi/10.1021/acs.nanolett.0c04015>.

Supplementary Figures S1 and S2 (PDF)

## ■ AUTHOR INFORMATION

### Corresponding Author

Yves F. Dufrene – Louvain Institute of Biomolecular Science and Technology, UCLouvain, B-1348 Louvain-la-Neuve, Belgium; [orcid.org/0000-0002-7289-4248](https://orcid.org/0000-0002-7289-4248);  
Email: [yves.dufrene@uclouvain.be](mailto:yves.dufrene@uclouvain.be)

### Authors

Marion Mathelié-Guinlet – Louvain Institute of Biomolecular Science and Technology, UCLouvain, B-1348 Louvain-la-Neuve, Belgium; [orcid.org/0000-0001-9023-3470](https://orcid.org/0000-0001-9023-3470)

Felipe Viela – Louvain Institute of Biomolecular Science and Technology, UCLouvain, B-1348 Louvain-la-Neuve, Belgium

Mariangela Jessica Alfeo – Department of Molecular Medicine, Unit of Biochemistry, University of Pavia, 27100 Pavia, Italy

Giampiero Pietrocola – Department of Molecular Medicine, Unit of Biochemistry, University of Pavia, 27100 Pavia, Italy; [orcid.org/0000-0002-7069-8155](https://orcid.org/0000-0002-7069-8155)

Pietro Speziale – Department of Molecular Medicine, Unit of Biochemistry, University of Pavia, 27100 Pavia, Italy

Complete contact information is available at:

<https://pubs.acs.org/10.1021/acs.nanolett.0c04015>

### Author Contributions

M.M.G., F.V., M.J.A., G.P., P.S., and Y.F.D. designed the experiments and wrote the article. M.M.G. and F.V. collected the data. M.M.G., F.V., and Y.F.D. analyzed the data.

### Notes

The authors declare no competing financial interest.

### ACKNOWLEDGMENTS

Work at the Université catholique de Louvain was supported by the European Research Council (ERC) under the European Union's Horizon 2020 research and innovation programme (693630), the National Fund for Scientific Research (FNRS), and the Research Department of the Communauté française de Belgique (Concerted Research Action). Y.F.D. is a Research Director at the FNRS.

### REFERENCES

- (1) Foster, T. J. The *Staphylococcus aureus* "Superbug". *J. Clin. Invest.* **2004**, *114* (12), 1693–1696.
- (2) Parlet, C. P.; Brown, M. M.; Horswill, A. R. Commensal *Staphylococcus aureus* Influence *Staphylococcus aureus* Skin Colonization and Disease. *Trends Microbiol.* **2019**, *27* (6), 497–507.
- (3) Thomer, L.; Schneewind, O.; Missiakas, D. Pathogenesis of *Staphylococcus aureus* Bloodstream Infections. *Annu. Rev. Pathol. Mech. Dis.* **2016**, *11*, 343–364.
- (4) Chambers, H. F.; Deleo, F. R. Waves of Resistance: *Staphylococcus aureus* in the Antibiotic Era. *Nat. Rev. Microbiol.* **2009**, *7* (9), 629–641.
- (5) Ogawa, S. K.; Yurberg, E. R.; Hatcher, V. B.; Levitt, M. A.; Lowy, F. D. Bacterial Adherence to Human Endothelial Cells in Vitro. *Infect. Immun.* **1985**, *50* (1), 218–224.
- (6) Menzies, B. E.; Kourteva, I. Internalization of *Staphylococcus aureus* by Endothelial Cells Induces Apoptosis. *Infect. Immun.* **1998**, *66* (12), 5994–5998.
- (7) Dziejwanowska, K.; Patti, J. M.; Deobald, C. F.; Bayles, K. W.; Trumble, W. R.; Bohach, G. A. Fibronectin Binding Protein and Host Cell Tyrosine Kinase Are Required for Internalization of *Staphylococcus aureus* by Epithelial Cells. *Infect. Immun.* **1999**, *67* (9), 4673–4678.
- (8) Sinha, B.; François, P. P.; Nüsse, O.; Foti, M.; Hartford, O. M.; Vaudaux, P.; Foster, T. J.; Lew, D. P.; Herrmann, M.; Krause, K. H. Fibronectin-Binding Protein Acts as *Staphylococcus aureus* Invasin via Fibronectin Bridging to Integrin  $\alpha_5\beta_1$ . *Cell. Microbiol.* **1999**, *1* (2), 101–117.
- (9) Hynes, R. O. Integrins: Bidirectional, Allosteric Signaling Machines. *Cell* **2002**, *110* (6), 673–687.
- (10) Sinha, B.; Herrmann, M. Mechanism and Consequences of Invasion of Endothelial Cells by *Staphylococcus aureus*. *Thromb. Haemostasis* **2005**, *94* (2), 266–277.
- (11) Edwards, A. M.; Potts, J. R.; Josefsson, E.; Massey, R. C. *Staphylococcus aureus* Host Cell Invasion and Virulence in Sepsis Is Facilitated by the Multiple Repeats within FnBPA. *PLoS Pathog.* **2010**, *6* (6), No. e1000964.
- (12) McDonnell, C. J.; Garcarena, C. D.; Watkin, R. L.; McHale, T. M.; McLoughlin, A.; Claes, J.; Verhamme, P.; Cummins, P. M.; Kerrigan, S. W. Inhibition of Major Integrin  $\alpha_V\beta_3$  Reduces *Staphylococcus aureus* Attachment to Sheared Human Endothelial Cells. *J. Thromb. Haemostasis* **2016**, *14* (12), 2536–2547.
- (13) Dersch, P.; Isberg, R. R. A Region of the *Yersinia pseudotuberculosis* Invasin Protein Enhances Integrin-Mediated Uptake into Mammalian Cells and Promotes Self-Association. *EMBO J.* **1999**, *18* (5), 1199–1213.
- (14) Dersch, P.; Isberg, R. R. An Immunoglobulin Superfamily-Like Domain Unique to the *Yersinia pseudotuberculosis* Invasin Protein Is Required for Stimulation of Bacterial Uptake via Integrin Receptors. *Infect. Immun.* **2000**, *68* (5), 2930–2938.
- (15) Mazmanian, S. K.; Skaar, E. P.; Gaspar, A. H.; Humayun, M.; Gornicki, P.; Jelenska, J.; Joachmiak, A.; Missiakas, D. M.; Schneewind, O. Passage of Heme-Iron across the Envelope of *Staphylococcus aureus*. *Science* **2003**, *299* (5608), 906–909.
- (16) Miajlovic, H.; Zapotoczna, M.; Geoghegan, J. A.; Kerrigan, S. W.; Speziale, P.; Foster, T. J. Direct Interaction of Iron-Regulated Surface Determinant IsdB of *Staphylococcus aureus* with the GPIIb/IIIa Receptor on Platelets. *Microbiology (London, U. K.)* **2010**, *156* (3), 920–928.
- (17) Zapotoczna, M.; Jevnikar, Z.; Miajlovic, H.; Kos, J.; Foster, T. J. Iron-Regulated Surface Determinant B (IsdB) Promotes *Staphylococcus aureus* Adherence to and Internalization by Non-Phagocytic Human Cells. *Cell. Microbiol.* **2013**, *15* (6), 1026–1041.
- (18) Ma, Y.-Q.; Qin, J.; Plow, E. F. Platelet Integrin  $\alpha_{IIb}\beta_3$ : Activation Mechanisms. *J. Thromb. Haemostasis* **2007**, *5* (7), 1345–1352.
- (19) Eliceiri, B. P.; Cheresh, D. A. The Role of  $\alpha_V$  Integrins during Angiogenesis: Insights into Potential Mechanisms of Action and Clinical Development. *J. Clin. Invest.* **1999**, *103* (9), 1227–1230.
- (20) Plow, E. F.; Haas, T. A.; Zhang, L.; Loftus, J.; Smith, J. W. Ligand Binding to Integrins. *J. Biol. Chem.* **2000**, *275* (29), 21785–21788.
- (21) Pietrocola, G.; Pellegrini, A.; Alfeo, M. J.; Marchese, L.; Foster, T. J.; Speziale, P. The Iron-Regulated Surface Determinant B (IsdB) Protein from *Staphylococcus aureus* Acts as a Receptor for the Host Protein Vitronectin. *J. Biol. Chem.* **2020**, *295* (29), 10008–10022.
- (22) Milles, L. F.; Gaub, H. E. Extreme Mechanical Stability in Protein Complexes. *Curr. Opin. Struct. Biol.* **2020**, *60*, 124–130.
- (23) Mathelié-Guinlet, M.; Viela, F.; Viljoen, A.; Dehullu, J.; Dufrière, Y. F. Single-Molecule Atomic Force Microscopy Studies of Microbial Pathogens. *Curr. Opin. Biomed. Eng.* **2019**, *12*, 1–7.
- (24) Viljoen, A.; Mignolet, J.; Viela, F.; Mathelié-Guinlet, M.; Dufrière, Y. F. How Microbes Use Force To Control Adhesion. *J. Bacteriol.* **2020**, *202* (12), 1.
- (25) Viela, F.; Mathelié-Guinlet, M.; Viljoen, A.; Dufrière, Y. F. What Makes Bacterial Pathogens so Sticky? *Mol. Microbiol.* **2020**, *113*, 683.
- (26) Friddle, R. W.; Noy, A.; De Yoreo, J. J. Interpreting the Widespread Nonlinear Force Spectra of Intermolecular Bonds. *Proc. Natl. Acad. Sci. U. S. A.* **2012**, *109* (34), 13573–13578.
- (27) Evans, E. Probing the Relation between Force–Lifetime—and Chemistry in Single Molecular Bonds. *Annu. Rev. Biophys. Biomol. Struct.* **2001**, *30*, 105–128.
- (28) Foster, T. J.; Geoghegan, J. A.; Ganesh, V. K.; Höök, M. Adhesion, Invasion and Evasion: The Many Functions of the Surface Proteins of *Staphylococcus aureus*. *Nat. Rev. Microbiol.* **2014**, *12* (1), 49–62.
- (29) Dufrière, Y. F.; Persat, A. Mechanobiology: How Bacteria Sense and Respond to Forces. *Nat. Rev. Microbiol.* **2020**, *18*, 227–240.
- (30) Viela, F.; Speziale, P.; Pietrocola, G.; Dufrière, Y. F. Mechanostability of the Fibrinogen Bridge between *Staphylococcus aureus* Surface Protein ClfA and Endothelial Cell Integrin  $\alpha_V\beta_3$ . *Nano Lett.* **2019**, *19* (10), 7400–7410.
- (31) Li, F.; Redick, S. D.; Erickson, H. P.; Moy, V. T. Force Measurements of the  $\alpha_5\beta_1$  Integrin-Fibronectin Interaction. *Biophys. J.* **2003**, *84* (2), 1252–1262.
- (32) Bharadwaj, M.; Strohmeyer, N.; Colo, G. P.; Helenius, J.; Beerenwinkel, N.; Schiller, H. B.; Fässler, R.; Müller, D. J.  $\alpha_V$ -Class Integrins Exert Dual Roles on  $\alpha_5\beta_1$  Integrins to Strengthen Adhesion to Fibronectin. *Nat. Commun.* **2017**, *8* (1), 14348.

- (33) Kong, F.; García, A. J.; Mould, A. P.; Humphries, M. J.; Zhu, C. Demonstration of Catch Bonds between an Integrin and Its Ligand. *J. Cell Biol.* **2009**, *185* (7), 1275–1284.
- (34) Strohmeyer, N.; Bharadwaj, M.; Costell, M.; Fässler, R.; Müller, D. J. Fibronectin-Bound  $\alpha5\beta1$  Integrins Sense Load and Signal to Reinforce Adhesion in Less than a Second. *Nat. Mater.* **2017**, *16* (12), 1262–1270.
- (35) Ponnuraj, K.; Bowden, M. G.; Davis, S.; Gurusiddappa, S.; Moore, D.; Choe, D.; Xu, Y.; Hook, M.; Narayana, S. V. L. A “Dock, Lock, and Latch” Structural Model for a Staphylococcal Adhesin Binding to Fibrinogen. *Cell* **2003**, *115* (2), 217–228.
- (36) Bowden, M. G.; Heuck, A. P.; Ponnuraj, K.; Kolosova, E.; Choe, D.; Gurusiddappa, S.; Narayana, S. V. L.; Johnson, A. E.; Höök, M. Evidence for the “Dock, Lock, and Latch” Ligand Binding Mechanism of the Staphylococcal Microbial Surface Component Recognizing Adhesive Matrix Molecules (MSCRAMM) SdrG. *J. Biol. Chem.* **2008**, *283* (1), 638–647.
- (37) Herman, P.; El-Kirat-Chatel, S.; Beaussart, A.; Geoghegan, J. A.; Foster, T. J.; Dufrene, Y. F. The Binding Force of the Staphylococcal Adhesin SdrG Is Remarkably Strong. *Mol. Microbiol.* **2014**, *93* (2), 356–368.
- (38) Herman-Bausier, P.; Labate, C.; Towell, A. M.; Derclaye, S.; Geoghegan, J. A.; Dufrene, Y. F. *Staphylococcus aureus* Clumping Factor A Is a Force-Sensitive Molecular Switch That Activates Bacterial Adhesion. *Proc. Natl. Acad. Sci. U. S. A.* **2018**, *115* (21), 5564–5569.
- (39) Milles, L. F.; Schulten, K.; Gaub, H. E.; Bernardi, R. C. Molecular Mechanism of Extreme Mechanostability in a Pathogen Adhesin. *Science* **2018**, *359* (6383), 1527–1533.
- (40) Vitry, P.; Valotteau, C.; Feuillie, C.; Bernard, S.; Alsteens, D.; Geoghegan, J. A.; Dufrene, Y. F. Force-Induced Strengthening of the Interaction between *Staphylococcus aureus* Clumping Factor B and Loricrin. *mBio* **2017**, *8* (6), No. e01748.
- (41) Marshall, B. T.; Long, M.; Piper, J. W.; Yago, T.; McEver, R. P.; Zhu, C. Direct Observation of Catch Bonds Involving Cell-Adhesion Molecules. *Nature* **2003**, *423* (6936), 190–193.
- (42) Le Trong, I.; Aprikian, P.; Kidd, B. A.; Forero-Shelton, M.; Tchesnokova, V.; Rajagopal, P.; Rodriguez, V.; Interlandi, G.; Klevit, R.; Vogel, V.; Stenkamp, R. E.; Sokurenko, E. V.; Thomas, W. E. Structural Basis for Mechanical Force Regulation of the Adhesin FimH via Finger Trap-like  $\beta$  Sheet Twisting. *Cell* **2010**, *141* (4), 645–655.
- (43) Yakovenko, O.; Sharma, S.; Forero, M.; Tchesnokova, V.; Aprikian, P.; Kidd, B.; Mach, A.; Vogel, V.; Sokurenko, E.; Thomas, W. E. FimH Forms Catch Bonds That Are Enhanced by Mechanical Force Due to Allosteric Regulation. *J. Biol. Chem.* **2008**, *283* (17), 11596–11605.
- (44) Thomas, W. E.; Trintchina, E.; Forero, M.; Vogel, V.; Sokurenko, E. V. Bacterial Adhesion to Target Cells Enhanced by Shear Force. *Cell* **2002**, *109* (7), 913–923.
- (45) Zhu, C.; Chen, W. Catch Bonds of Integrin/Ligand Interactions. In *Single-molecule Studies of Proteins*; Oberhauser, A. F., Ed.; Springer, 2013; pp 77–96.
- (46) Zhu, C.; Chen, Y.; Ju, L. A. Dynamic Bonds and Their Roles in Mechanosensing. *Curr. Opin. Chem. Biol.* **2019**, *53*, 88–97.
- (47) Prezhdo, O. V.; Pereverzev, Y. V. Theoretical Aspects of the Biological Catch Bond. *Acc. Chem. Res.* **2009**, *42* (6), 693–703.
- (48) Thomas, W. E.; Vogel, V.; Sokurenko, E. Biophysics of Catch Bonds. *Annu. Rev. Biophys.* **2008**, *37* (1), 399–416.
- (49) Sokurenko, E. V.; Vogel, V.; Thomas, W. E. Catch-Bond Mechanism of Force-Enhanced Adhesion: Counterintuitive, Elusive, but ... Widespread? *Cell Host Microbe* **2008**, *4* (4), 314–323.
- (50) Chakrabarti, S.; Hinczewski, M.; Thirumalai, D. Plasticity of Hydrogen Bond Networks Regulates Mechanochemistry of Cell Adhesion Complexes. *Proc. Natl. Acad. Sci. U. S. A.* **2014**, *111* (25), 9048–9053.
- (51) Otto, M. Physical Stress and Bacterial Colonization. *FEMS Microbiol. Rev.* **2014**, *38* (6), 1250–1270.
- (52) Beaussart, A.; El-Kirat-Chatel, S.; Sullan, R. M. A.; Alsteens, D.; Herman, P.; Derclaye, S.; Dufrene, Y. F. Quantifying the Forces Guiding Microbial Cell Adhesion Using Single-Cell Force Spectroscopy. *Nat. Protoc.* **2014**, *9* (5), 1049–1055.